Angewandte Chemie
Eine Zeitschrift der Gesellschaft Deutscher Chemiker

Supporting Information

High-Pressure NiAs-Type Modification of FeN

*William P. Clark, Simon Steinberg, Richard Dronskowski, Catherine McCammon, Ilya Kupenko, Maxim Bykov, Leonid Dubrovinsky, Lev G. Akselrud, Ulrich Schwarz, and Rainer Niewa**

anie_201702440_sm_miscellaneous_information.pdf

Supporting Information

Table of Contents

1. Experimental Procedures

1.1 Synthesis of ζ-$^{57}Fe_2N$

The starting material was a ^{57}Fe-enriched sample of ζ-Fe_2N. Due to the risk of oxygen and water contamination, all of the preparations were conducted within an argon filled glove box. The starting material was produced by placing ^{57}Fe powder in a corundum boat and inserted into a quartz tube. The reagent was then heated to 413 °C, within 2 hours, for 60 hours under a constant flow of ammonia (99.999%, Linde, 60 sccm). The temperature was then lowered over 6 hours to 113 °C, before being allowed to cool to ambient temperature.[1] The product was confirmed by powder X-Ray diffraction to be single-phase ζ-$^{57}Fe_2N$.
The starting material was analyzed using a STOE STADI P equipped with a Mythen1K micro-strip detector in transmission geometry, using Mo-Kα1 radiation (λ = 70.93 pm).

1.2 Experimental equipment and conditions

The combination of laser heated diamond anvil cells and synchrotron Mössbauer source spectroscopy were used to investigate phase formations of the two samples, above 1000 K and under pressures of up to 45 GPa at the Nuclear Resonance beamline (ID18 beam-line at ESRF).

X-ray diffraction patterns were measured using synchrotron radiation (ID09 beam-line at ESRF, X-ray wavelength 0.415054 Å with beamsize about 10 mkm FWHM).

1.3 Computational Method

Full structural optimizations as well as electronic band structure computations, chemical bonding analyses and phonon band structure calculations were carried out with the projector augmented wave method[2] (VASP code),[3] a variant of the COHP technique[4] (LOBSTER code)[5] and the ab initio force[6] constant procedure (PHONOPY code),[7] respectively.

2. Results and Discussion

2.1 Mössbauer Data

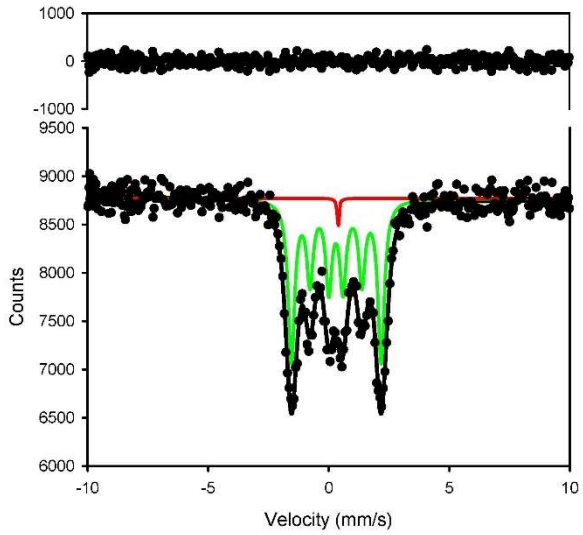

Figure S1. ^{57}Fe-Mössbauer spectra of ^{57}Fe in N_2 pressure medium, after annealing, at 11.9 GPa

2.2 Refined Crystal Data

The refinements were conducted using the FULLPROF[8] program. During refinement the following parameters were allowed to be refined: scale factor, zero shift, three coefficients from the background polynomial, unit cell parameters, three reflections widths (*u*, *v* and *w*), isotropic thermal displacement parameters and two asymmetry parameters.

Table S1. Crystal structural data of FeN, at different pressures after refinement in the NiAs structure.

Pressure	**13.3 GPa**	**4.4 GPa**	**0.1 MPa**
***a* (Å)**	2.737(3)	2.775(7)	2.800(2)
***c* (Å)**	4.933(5)	4.982(1)	5.015(5)
***V* (Å^3)**	32.005	33.241	34.050
***c*/*a* ratio**	1.802	1.795	1.791
Space Group	$P6_3/mmc$		
	Wyckoff Positions	**Atomic Positions**	
Fe	2*a*	0, 0, 0	
N	2*c*	⅓, ⅔, ¼	

2.3 Computational Details

The electronic and the phonon band structures of the NiAs-type FeN were investigated to provide an insight into the electronic and the vibrational properties of this material. Additionally, the total energies and pressure-dependent enthalpies of the NiAs-type FeN were determined and compared to those of the ZnS-type FeN, which, according to previous quantum chemical examinations on the Fe−N system,[9] is expected to be the electronically and dynamically most favorable modification of FeN. From the comparisons of the total energies and the pressure-dependent relative enthalpies for both the NiAs-type and the ZnS-type FeN it is achievable to evaluate the stability of the NiAs-type FeN relative to the ZnS-type modification.

All electronic band structure calculations and full structural optimizations including lattice parameters and atomic positions for both modifications of FeN were performed utilizing the projector augmented wave method of Blöchl[2] as implanted in the *Vienna ab-initio Simulation Package* (VASP) by Kresse and Joubert.[3] Because the Mössbauer spectra of the NiAs-type FeN indicate a magnetic ground state for this material, non-magnetic, ferromagnetic and antiferromagnetic models of the NiAs-type FeN were examined to elucidate the nature and the origin of the magnetic characteristics. Additionally, the total energies and the pressure-dependent enthalpies of the ferromagnetic NiAs-type FeN model that corresponds to the lowest total energy among all inspected NiAs-type FeN models were compared to those of the ZnS-type FeN, for which, based on previous proposals on the magnetic ground state of this material,[10] an antiferromagnetic starting model was employed.

Correlation and exchange in all computations were described by the generalized gradient approximation of Perdew, Burke and Ernzerhof (GGA−PBE),[11] while sets of 16 × 16 × 16 and 20 × 20 × 10 *k*-points were used to sample the first Brillouin zones in the ZnS-type and the NiAs-type FeN, respectively, for reciprocal space integrations. The energy cutoff of the plane wave basis set was 400 eV and all computations converged until the energy differences fell below 10^{-8} (10^{-6}) eV/cell between two iterative steps of the electronic (and the ionic) relaxation.

Chemical bonding analyses for the ZnS-type and the NiAs-type FeN were accomplished based on a variant of the crystal orbital Hamilton population (−COHP) technique, in which the off-site projected densities-of-states (DOS) are weighted by the respective Hamilton matrix elements to indicate antibonding, non-bonding and bonding interactions.[12] Although this method requires the use of crystal orbitals derived from local basis sets, yet, the herein employed projected –COHP (−pCOHP) technique, a derivative of the aforementioned −COHP method,[4] enables to obtain the Hamilton-weighted populations from the results of plane-wave-based electronic structure calculations. The Hamilton-weighted populations were developed from the plane-wave basis sets with the aid of the *Local-Orbital Basis Suite Towards Electronic-Structure Reconstruction* software package (LOBSTER-2.0.0[4,5,12]).

The vibrational properties of the ferromagnetic NiAs-type FeN model were evaluated from the phonon band structure and density-of-states (PhDOS), which were calculated utilizing the *ab initio* force constant method[6] within the *PHONOPY* code.[7] In particular, the phonon frequencies were determined from force constant matrices, for which the interatomic forces within supercells corresponding to 7 × 7 × 4 expansions of the original unit cell were computed using VASP in the Γ-point approximation (this methodological approach has already been employed successfully elsewhere[13]).

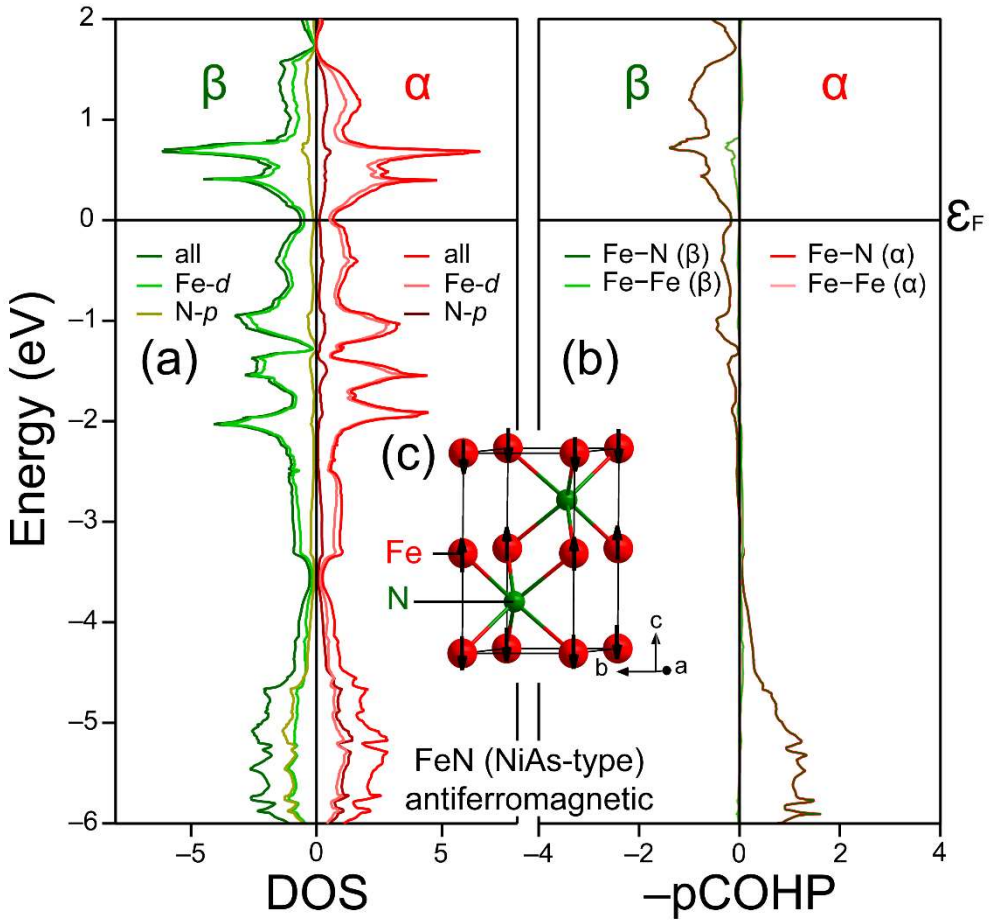

Figure S2. (a) Spin-polarized DOS and **(b)** –pCOHP curve of the antiferromagnetic NiAs-type FeN model: the horizontal line represents the Fermi level, E_F, and a representation of the antiferromagnetic NiAs-type FeN model is shown in the inset **(c)**.

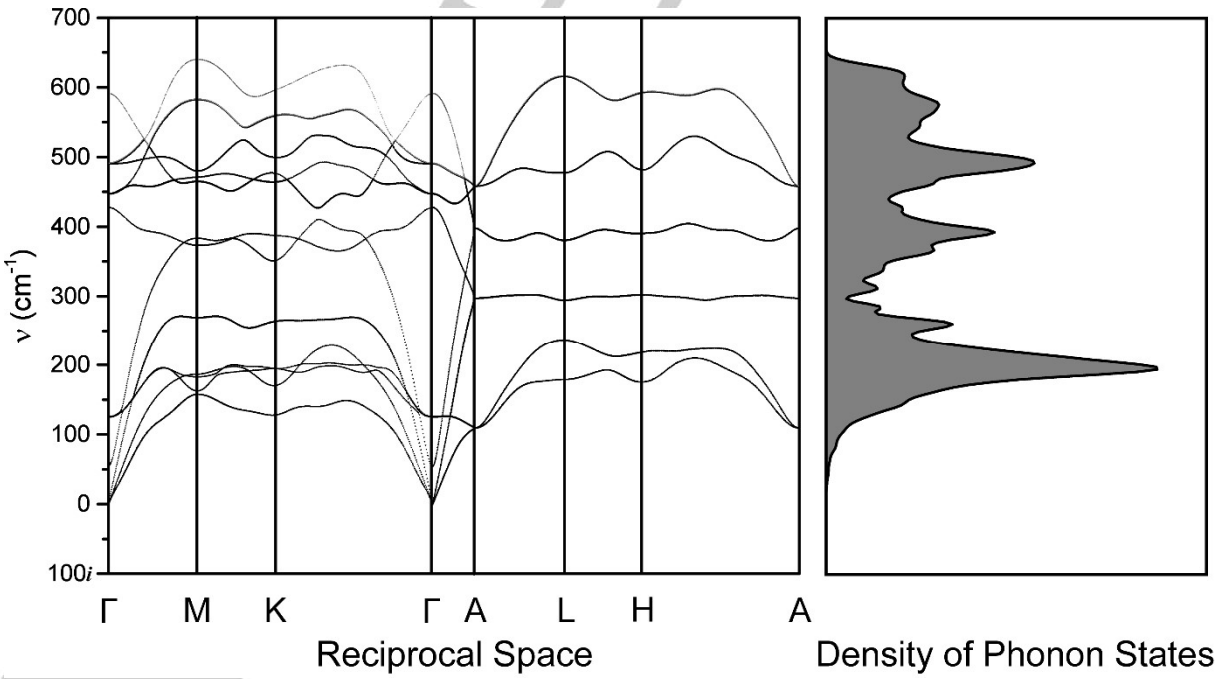

Figure S3. Phonon band structure and density-of-state curve of the NiAs-type FeN: note that imaginary wavenumbers that are signs of dynamic instabilities are not evident in the frequencies of the phonon band structure. The interatomic forces were evaluated from spin-polarized computations, for which the projector augmented wave method (see Computational Details) was employed.

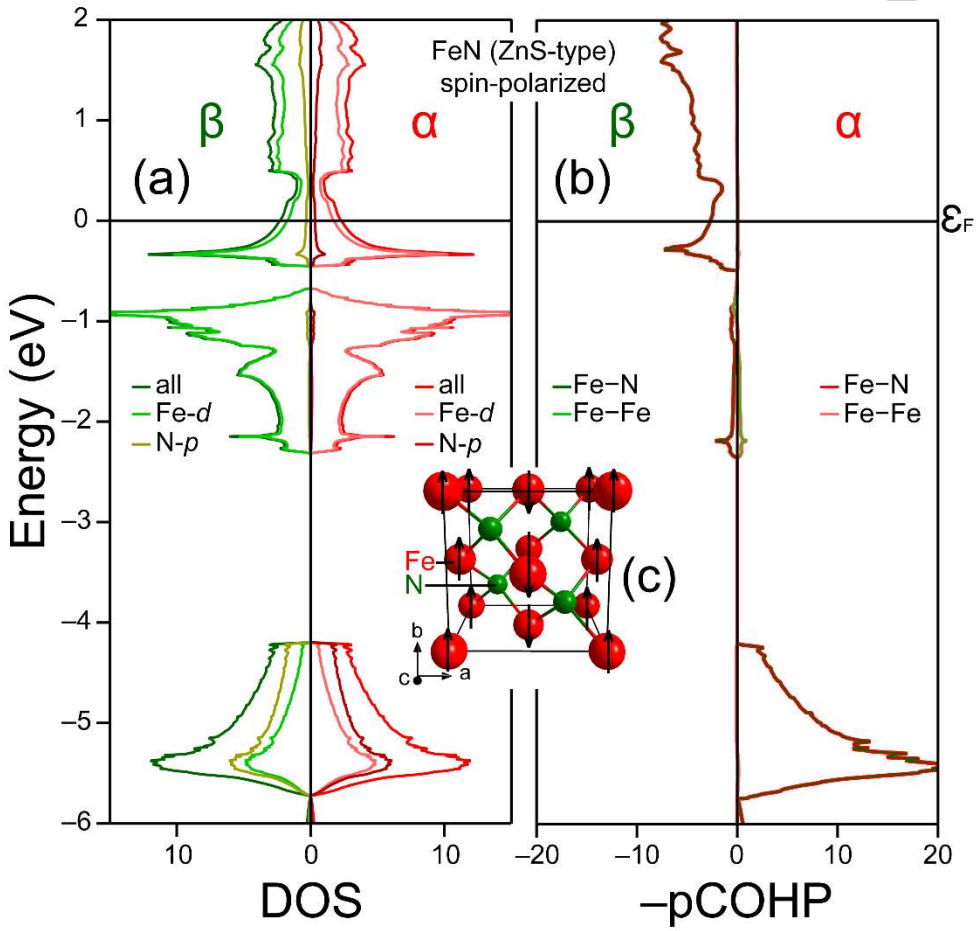

Figure S4. (a) Spin-polarized DOS and **(b)** –pCOHP curves of the ZnS-type FeN, for which an antiferromagnetic starting model was employed: a representation of the starting model is shown in the inset **(c)** and the Fermi level, E_F, is represented by the horizontal line. The vibrational properties of the ZnS-type FeN have been examined elsewhere.[1a]

Table S2. Integrated projected Crystal Orbital Hamilton Population (−IpCOHP) values, distances and multiplicities of selected contacts in the ZnS-type FeN, for which an antiferromagnetic starting model was employed, and the ferromagnetic as well as antiferromagnetic NiAs-type FeN models.

Interaction	Distance (Å)	Multiplicity	IpCOHP (eF)	
			Spin 1	Spin 2
FeN (NiAs-type), ferromagnetic model				
Fe1−N3	2.01321	3	−1.07849	−1.26787
Fe1−N4	2.01321	3	−1.07926	−1.26813
Fe2−N3	2.01321	3	−1.07904	−1.26742
Fe2−N4	2.01321	3	−1.07824	−1.26720
Fe1−Fe2	2.49875	2	−0.15062	−0.28814
FeN (NiAs-type), antiferromagnetic model				
Fe1−N3	2.01719	3	−1.03085	−1.29270
Fe1−N4	2.01719	3	−1.03041	−1.29301
Fe2−N3	2.01719	3	−1.29266	−1.03077
Fe2−N4	2.01719	3	−1.29310	−1.03044
Fe1−Fe2	2.47591	2	−0.24777	−0.24782
FeN (ZnS-type)				
Fe1−N5	1.83262	1	−1.86734	−1.86238
Fe1−N6	1.83262	1	−1.86214	−1.86205
Fe1−N7	1.83262	1	−1.86246	−1.85726
Fe1−N8	1.83262	1	−1.86190	−1.86253
Fe2−N5	1.83262	1	−1.85623	−1.86344
Fe2−N6	1.83262	1	−1.85656	−1.86766
Fe2−N7	1.83262	1	−1.86306	−1.86655
Fe2−N8	1.83262	1	−1.85693	−1.86716
Fe3−N5	1.83262	1	−1.86127	−1.86298
Fe3−N6	1.83262	1	−1.86279	−1.85688
Fe3−N7	1.83262	1	−1.86257	−1.86158
Fe3−N8	1.83262	1	−1.86861	−1.86109
Fe4−N5	1.83262	1	−1.86125	−1.86294
Fe4−N6	1.83262	1	−1.86823	−1.86150
Fe4−N7	1.83262	1	−1.86194	−1.86243
Fe4−N8	1.83262	1	−1.86246	−1.85734
Fe1−Fe2	2.99265	4	−0.09757	−0.09735
Fe1−Fe3	2.99265	4	−0.09735	−0.09757
Fe1−Fe4	2.99265	4	−0.09736	−0.09754
Fe2−Fe3	2.99265	4	−0.09756	−0.09738
Fe2−Fe4	2.99265	4	−0.09757	−0.09735
Fe3−Fe4	2.99265	4	−0.09735	−0.09757

3. References

[1] M. Widenmeyer, T. C. Hansen, E. Meissner, R. Niewa, *Z. Anorg. Allg. Chem.* **2014**, *640*, 1265.

[2] J. Lehtomäki, I. Makkonen, M. A. Caro, A. Harju, O. Lopez-Acevedo, *Phys. Rev. B* **2014**, *50*, 17953.

[3] a) G. Kresse, M. Marsmann, J. Furthmüller, *Vienna Ab Initio Simulation Package (VASP), The Guide*, Computational Materials Physics, Faculty of Physics, Universität Wien, Vienna, Austria, **2014**; b) G. Kresse, J. Furthmüller, *Comput. Mater. Sci.* **1996**, *6*, 15; c) G. Kresse, J. Furthmüller, *Phys. Rev. B* **1996**, *54*, 11169; d) G. Kresse, J. Hafner, *Phys. Rev. B* **1993**, *47*, 558; e) G. Kresse, D. Joubert, *Phys. Rev. B* **1999**, *59*, 1758.

[4] V. L. Deringer, A. L. Tchougréeff, R. Dronskowski, *J. Phys. Chem. A* **2011**, *115*, 5461.

[5] a) S. Maintz, V. L. Deringer, A. L. Tchougréeff, R. Dronskowski, *J. Comput. Chem.* **2013**, *34*, 2557; b) S. Maintz, V. L. Deringer, A. L. Tchougréeff, R. Dronskowski, *J. Comput. Chem.* **2016**, *37*, 1030.

[6] K. Parlinski, Z. Q. Li, Y. Kawazoe, *Phys. Rev. Lett.* **1997**, *78*, 4063.

[7] A. Togo, F. Oba, I. Tanaka, *Phys. Rev. B.* **2008**, *78*, 1.

[8] J. Rodriguez-Carvajal, FULLPROF2.k, Version 5.3, Mar2012-ILL-JRC, **2012**.

[9] a) H. R. Soni, V. Mankad, S. K. Gupta, P. K. Jha, *J. Alloy. Compd.* **2012**, *522*, 106; b) B. Eck, R. Dronskowski, M. Takahashi, S. Kikkawa, *J. Mater. Chem.* **1999**, *9*, 1527.

[10] K. Suzuki, H. Morita, T. Kaneko, H. Yoshida, H. Fujimori, *J. Alloy. Compd.* **1993**, *201*, 11.

[11] J. P. Perdew, K. Burke, Y. Wang, *Phys. Rev. B* **1996**, *54*, 16533.

[12] R. Dronskowski, P. E. Bloechl, *J. Phys. Chem.* **1993**, *97*, 8617.

[13] V. L. Deringer, R. P. Stoffel, M. Wuttig, R. Dronskowski, *Chem. Sci.* **2015**, *6*, 5255.